Proc. Natl. Acad. Sci. USA
Vol. 91, pp. 8690–8694, August 1994
Neurobiology

Functional magnetic resonance imaging of human prefrontal cortex activation during a spatial working memory task

(echo-planar imaging/magnetic susceptibility)

GREGORY MCCARTHY*†, ANDREW M. BLAMIRE†, AINA PUCE*†, ANNA C. NOBRE*†, GILLES BLOCH‡§, FAHMEED HYDER¶, PATRICIA GOLDMAN-RAKIC‖, AND ROBERT G. SHULMAN‡

*Neuropsychology Laboratory 116B1, Veterans Affairs Medical Center, West Haven, CT 06516; and Departments of †Surgery (Neurosurgery), ‡Molecular Biophysics and Biochemistry, ¶Chemistry, and ‖Neurobiology, Yale University School of Medicine, New Haven, CT 06510

Contributed by Robert G. Shulman, April 25, 1994

ABSTRACT **High-speed magnetic resonance (MR) imaging was used to detect activation in the human prefrontal cortex induced by a spatial working memory task modeled on those used to elucidate neuronal circuits in nonhuman primates. Subjects were required to judge whether the location occupied by the current stimulus had been occupied previously over a sequence of 14 or 15 stimuli presented in various locations. Control tasks were similar in all essential respects, except that the subject's task was to detect when one of the stimuli presented was colored red (color detection) or when a dot briefly appeared within the stimulus (dot detection). In all tasks, two to three target events occurred randomly. The MR signal increased in an area of the middle frontal gyrus corresponding to Brodmann's area 46 in all eight subjects performing the spatial working memory task. Right hemisphere activation was greater and more consistent than left. The MR signal change occurred within 6–9 sec of task onset and declined within a similar period after task completion. An increase in MR signal was also noted in the control tasks, but the magnitude of change was less than that recorded in the working memory task. These differences were replicated when testing was repeated in five of the original subjects. The localization of spatial working memory function in humans to a circumscribed area of the middle frontal gyrus supports the compartmentalization of working memory functions in the human prefrontal cortex and the localization of spatial memory processes to comparable areas in humans and nonhuman primates.**

Working memory (1) provides temporary storage of information for cognitive capacities including comprehension and reasoning. The neural substrates for working memory have been elucidated in studies of nonhuman primates (2). Spatial working memory tasks requiring the brief storage of spatial information throughout the visual field engage neurons in the principal sulcus in the mid-dorsolateral cortex of rhesus monkeys (3, 4). Individual neurons in this region increase their discharge for particular target locations as monkeys recall the position of a previous stimulus (memory fields) (5). The same region is innervated by cortico–cortical projections from the posterior parietal cortex (6), where spatial perceptions are consolidated (7). These studies suggest that areas of the dorsolateral prefrontal cortex, by virtue of their extrinsic connections and physiological properties, are specialized for processing of spatial information in working memory.

Positron emission tomography (PET) has recently been used to study working memory in humans. Petrides *et al.* (8) found that object working memory using pictures activated a region of the right middle frontal gyrus, including Brodmann's area 9 and 46 and that these regions were activated bilaterally by a verbal working memory task (9). On the other hand, Paulescu *et al.* (10) found more posterior frontal activation in Broca's area (area 44) and parietal cortex (area 40) in a verbal working memory task. Jonides *et al.* (11) reported activation in inferior frontal cortex (Brodmann's area 47) and posterior parietal cortex during a spatial working memory task. The reasons for the differences among human studies and the lack of correspondence of some studies with nonhuman primate research are not well understood but may, in part, be due to the influence of verbal strategies.

The present study reinvestigates the role of the dorsolateral prefrontal cortex in spatial working memory using the method of functional magnetic resonance (MR) imaging (fMRI). The fMRI method has been shown by us (12) and others (13) to be a sensitive indicator of neural function, while providing good anatomical and temporal resolution. We have used a design that taxes spatial working memory capacity while discouraging verbal strategies. Preliminary reports of these data have been presented in abstract form (14, 15).

MATERIALS AND METHODS

Subjects. Eight subjects (four females) participated in the main experiment. Five subjects were retested to obtain data on reliability. Each session lasted 2.5–3 hr. The experimental protocol was approved by the Yale Human Investigations Committee, and all subjects provided informed consent.

Working Memory Task. Three behavioral tasks employed identical visual stimuli presented against a dark background with a central fixation cross. In the spatial working memory task ("Location"), subjects were presented with white irregular stimuli that appeared at different locations. Each run consisted of 14–15 stimuli presented at a rate of one per 1.5 sec. The stimuli for each run were randomly chosen from 20 different designs and 20 spatial locations. The stimuli were chosen not to suggest nameable objects and were white, except for two to three per run that were colored red. The pattern of locations was irregular, so that subjects would not attach verbal labels to spatial positions. The subject raised an index finger whenever a shape appeared in a location previously occupied during that same run. There were two to three such target events per run. Neither shape nor color was relevant.

Control Tasks. Similar stimuli, locations, and timing were used in the control tasks. In the "Color" target detection

The publication costs of this article were defrayed in part by page charge payment. This article must therefore be hereby marked "*advertisement*" in accordance with 18 U.S.C. §1734 solely to indicate this fact.

Abbreviations: EPI, echo-planar imaging; MR, magnetic resonance; fMRI, functional MR imaging; PET, positron emission tomography; ROI, region of interest; T_1, longitudinal relaxation time; *TR*, repetition time; *TE*, echo time.

§Present address: Service Hospitalier Frederic Joliot, Department Pharmacologie et Physiologie, 4, Place Du Gal LeClerc, 91406 Orsay, France.

task, subjects made a finger response whenever a red shape appeared. Spatial location was irrelevant. In the "Dot" target detection task, subjects responded whenever a small dot briefly appeared within a shape. The dot's onset was random, thus requiring subjects to attend to a shape during its entire 1500-ms duration. Both control tasks were sensory-guided, but the Dot task required constant attention to the stimuli and was more difficult than the Color control task. In an additional "Baseline" control task, subjects were instructed to relax with eyes open during image acquisition.

The Location and control tasks were randomly grouped and repeated three to six times within each session. Each task occurred with equal frequency over the course of the imaging session. Control tasks occurred in close temporal proximity to the primary spatial working memory task. The Dot task was added in the replication study.

The experimental tasks were controlled by a laptop computer using the MEL software system (Psychology Software Tools, Pittsburgh). Stimuli were displayed on a liquid crystal display panel (Sharp Instruments) and projected onto a screen at the end of the patient gurney. The subjects viewed the screen with prism glasses. To insure stable performance, subjects practiced the Location task during the 1- to 1.5-hr set-up time.

Imaging Sequence. All images were obtained at 2.1 T on a Bruker Biospec spectrometer using a linear bird-cage resonator. Scout MR images were acquired in sagittal planes about the midline using a four-plane multislice inversion recovery sequence to give good gray–white matter contrast [slice thickness = 5 mm, separation = 7 mm, repetition time (*TR*) = 2100 ms, echo time (*TE*) = 17 ms, inversion time = 760 ms, matrix = 128^2]. Scout images were acquired in the coronal plane about a point 4 cm anterior to the anterior commissure using the above sequence. This slice was selected to include Brodmann's area 46 and 9 within the middle frontal gyrus (16).

Localized shimming of the slice was done (17) to maximize the magnetic field homogeneity and hence the functional signal changes. To establish the location of major vessels, a single-slice time-of-flight angiogram was acquired (slice thickness = 5 mm, *TR* = 70 ms, *TE* = 17 ms, flip angle = 45°). With these parameters, the angiogram depicted mainly vessels with high flow rates.

Coronal functional MR images were acquired using the echo-planar imaging (EPI) sequence (18). The first study on each subject was performed with an asymmetric spin-echo version of EPI which generated a spin-echo from the slice followed by a gradient echo delay (*TE*) of 50 ms for evolution of functional signal changes (19). Images in the second session were acquired using a gradient-echo version of EPI (*TE* = 50 ms and added cerebrospinal fluid suppression using an adiabatic inversion pulse and inversion time of 2040 ms). In both cases lipid signals from the scalp were suppressed. Slice thickness was 10 mm, and nominal in-plane resolution was 6 × 3 mm with a matrix of 64^2.

One run of each task consisted of a time series of 32 echo-planar images (*TR* = 3000 ms), which included three intervals: pretask (images 1–12), task (images 13–22), and posttask (images 23–32). Four additional scans were acquired before the time series to achieve steady-state transverse magnetization.

Artifact Detection. Before further analysis, the center of mass of each image within each run was calculated. Deviations in this measure and examinations of runs in a cine loop were used to identify movement and other artifacts. With these procedures, 15 of 172 runs were eliminated from further analyses.

Data Analysis. A multistep analysis procedure was developed based upon our prior studies (12, 19). (*i*) A *t*-test image comparing the pretask and task intervals (images 1–12 vs. 14–22) was calculated for each run. The task interval was offset by 6 sec (i.e., two images) from the actual duration of the task (images 12–20), as our prior studies had shown a delay of ≈6 sec in the MR activation response. (*ii*) For each subject, individual *t*-test images were combined into a mean *t*-test image for each task. These mean *t*-test images retained only *t* values above a specified criterion and were superimposed upon corresponding anatomical images. The *t* threshold criteria varied between 3.0 and 4.0 across subjects due to different signal/noise levels, but the same criterion was always used for comparison of tasks *within* each subject. (*iii*) An AND *t*-test image was computed for each subject in which the *t*-test images for each task were combined such that only voxels exceeding a specified *t* value ($t = 1.5$, $P < 0.05$) in *all* runs were retained. (*iv*) Clusters of activated voxels were identified in the thresholded mean *t*-test images for each subject and task. These regions of interest (ROIs) were interrogated for each image in each run, such that an average time course of activation could be determined. The time course of activation was scaled to represent percentage signal change (or ΔS) relative to the mean of the pretask images. (*v*) A grand mean *t*-test image was calculated across all subjects. All images were first aligned to a representative subject whose anatomy approximated that of the corresponding level in the Talairach atlas (16). A "blind" observer determined scaling and translation factors separately for the *x* and *y* dimensions to align each individual's anatomical image to the standard. A grand-mean *t*-test image was then computed for each task by averaging each individual's *t*-test images in this common dimensional space. (*vi*) Anatomical ROIs were computed in which the gray matter bounding the middle frontal gyri (encompassing area 46) was outlined and used for image interrogation in each run, as described in step *iv* above.

RESULTS

Fig. 1 represents data from subject AAH. In Fig. 1*A*, the mean *t*-test image for Location (thresholded at $t \geq 3.25$) represents voxels in the echo-planar image in which signal intensity increased significantly during performance of the Location task relative to the pretask interval. The AND *t* image (data not shown) showed the same ROI. The activation occurred in the right middle frontal gyrus. No other area in the slice was activated above pretask levels. Note that the anatomical resolution of the activation effect is less precise than that of the T_1-weighted image because the echo-planar voxels are larger.

Fig. 1*C* presents the average time course of activation for subject AAH for the single activated cluster (Fig. 1*A*) for both Location and Color. Note that change in signal intensity exceeds pretask noise levels within 3–6 sec after onset for the Location task and reaches a peak activation increase of ≈2.6% by 9 sec. The activation declines immediately after the task cessation but requires ≈15 sec to reach pretask levels. The time course for Color shows a similar profile, but the activation level reached is approximately half that of Location ($P < 0.0001$).

An anatomically based ROI was defined by outlining the gray matter for the right middle frontal gyrus. This was done to determine whether using the ROI based on the Location *t* image was underestimating the strength of activation for Color. The anatomical ROI and activation time courses are shown in Fig. 1*B* and *D*, respectively. Similar time courses were observed for both Location and Color. Greater activation was obtained in Location ($P < 0.0001$).

Fig. 2 presents data for subject APE's first session in which the mean *t*-test image for Location (thresholded at $t \geq 3.00$) shows two clusters of activated voxels, one cluster in each of the right and left middle frontal gyri. Significant activation of ≈5% occurred in Location. Smaller activation was also

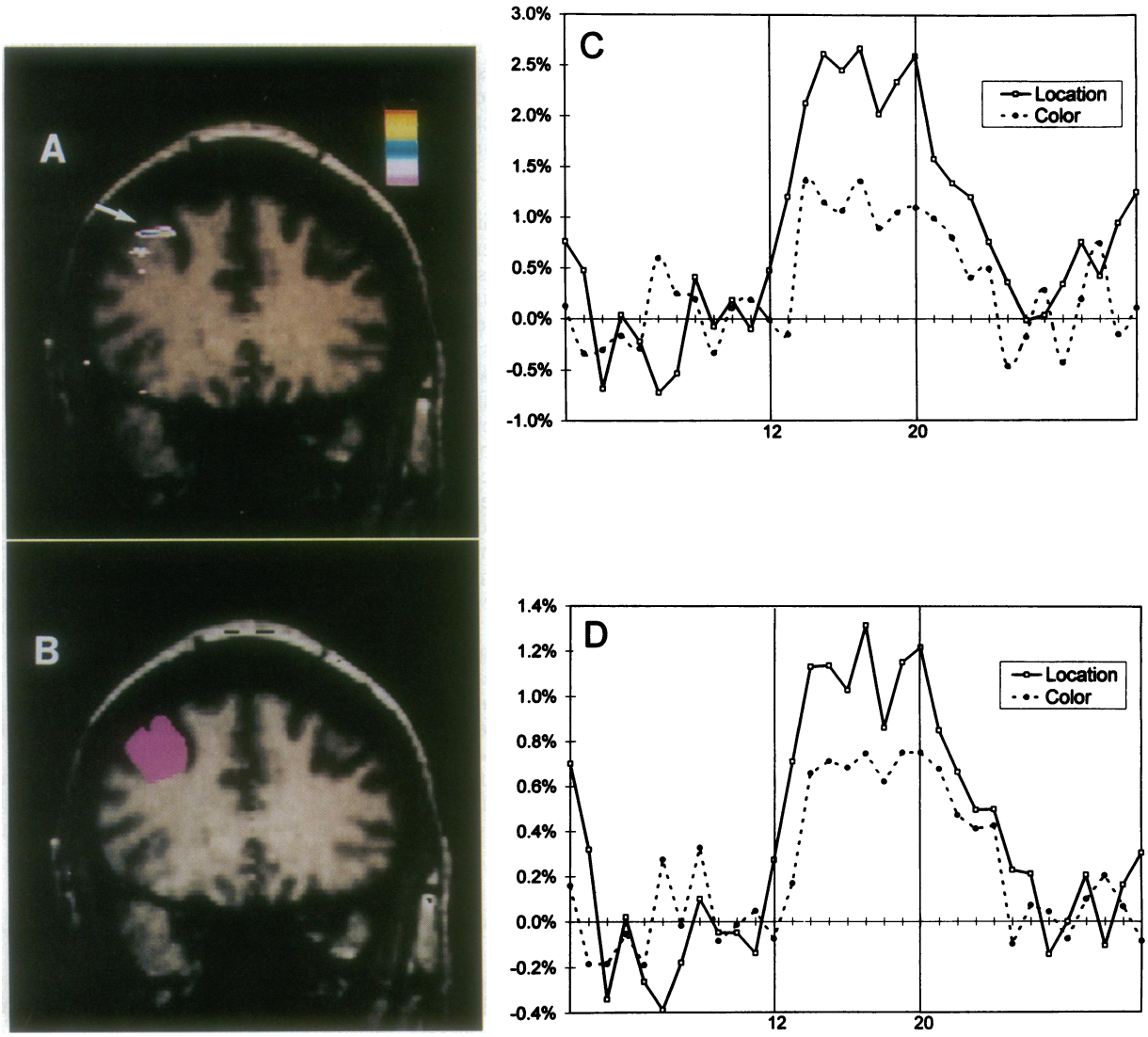

FIG. 1. Subject AAH. (*A*) Mean *t*-test image for Location task superimposed upon a longitudinal relaxation time (T_1) weighted anatomical image. Arrow indicates focus of activation. (Note, in this and all subsequent images, the right side of the brain appears on the left side of the image.) The color scale indicates increasing *t* values from violet to red beginning at the specified threshold. (*B*) Anatomically based ROI outlining of gray matter of the right middle frontal gyrus. (*C*) Average time course of activation for the ROI in the right middle frontal gyrus shown in *A* for Location and Color tasks. In this and all subsequent plots, the *x* axis shows the image number in the time series, and the *y* axis depicts the percentage signal change between task and pretask period divided by the mean pretask signal (i.e., $\Delta S/S$). The vertical lines at images 12 and 20 indicate the beginning and end of the task. (*D*) Average activation time course for the ROI displayed in *B*. Note the change in scale of the *y* axis.

observed in Color ($P < 0.016$ for left and $P < 0.011$ for right hemisphere). No activation was observed in Baseline. Anatomical ROIs were traced for each middle frontal gyrus. In both gyri, significant overall activation was obtained, and Location showed greater activation than Color ($P < 0.003$ for right and $P < 0.001$ for left hemisphere). The remainder of the subjects in the first session showed consistent activation in the middle frontal gyri for Location. Other regions also showed activation but not consistently across subjects.

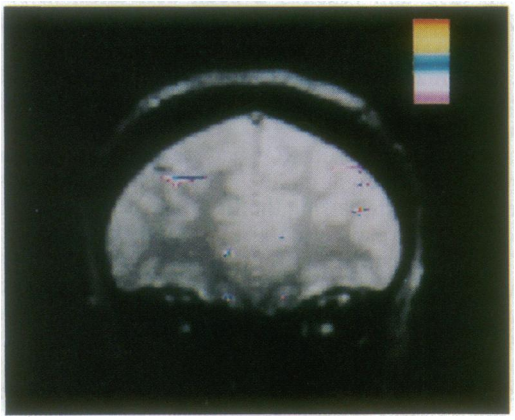

FIG. 2. Subject APE, first test session. Mean *t*-test image for Location task superimposed upon anatomical image.

To represent consistent findings across subjects, intersubject grand mean *t*-test images were calculated (see *v* in the Data Analysis section of *Materials and Methods*). A small cluster of activation is seen in the right middle frontal gyrus for Location group data (Fig. 3*A*) similar to that seen in the individual data of subjects AAH and APE above. A smaller midline cluster of activation is also visible near the cingulate gyrus. No additional clusters were obtained ($t \geq 1.5$ threshold); however, a small cluster could be seen in the left middle frontal gyrus when the *t* threshold was lowered. Fig. 3*B* presents the grand mean *t*-test image for Color. A small cluster is visible in the right frontal region somewhat ventral to that seen in Location. As the *t*-test images were computed identically for each task and displayed by using the same

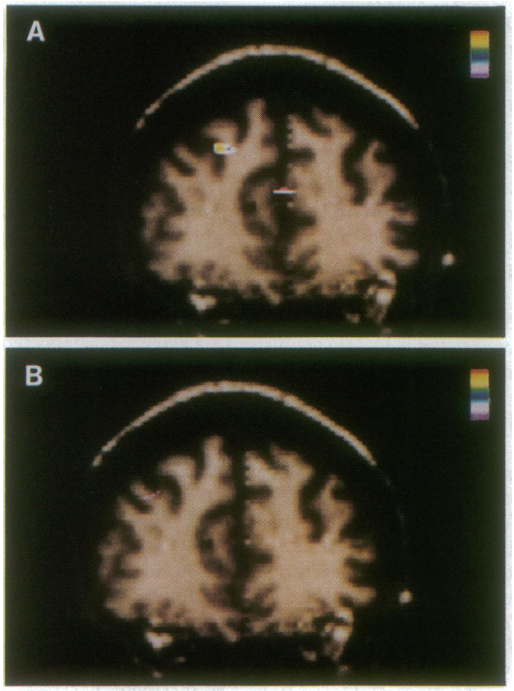

FIG. 3. (*A*) Grand mean *t*-test image for Location task across eight subjects studied in the first test session showing activation in the right middle frontal region and cingulate cortex. These group data have been superimposed upon a single subject's anatomical T_1-weighted image. (*B*) Corresponding grand mean *t*-test image for Color task across eight subjects showing minimal activation in the right middle frontal region.

threshold, the relative degree of activation for each task can be directly compared in these figures. No activation was seen in the Baseline condition (data not shown).

Five subjects participated in a replication study several weeks later. A gradient echo EPI sequence was used with an inversion recovery pulse to suppress the cerebrospinal fluid signal. The Dot task was also introduced in this session. Fig. 4 presents the second-session data for subject APE (see Fig. 2). In this session, the contrast in the T_1-weighted anatomical image was different. The shimmed echo-planar image was asymmetric with some signal loss from the left hemisphere. The mean *t*-test image ($t > 4.0$) for Location is shown in Fig. 4, where a strong activation was found in the right middle frontal gyrus. Location produced a 3.5% signal increase, which was significantly greater than the activation produced by either Dot ($P < 0.0035$) or Color ($P < 0.001$).

Grand mean *t*-test images were computed for the replication study. Fig. 5 *A* and *B* represents the results of Location and Color, respectively. The same region in the right middle

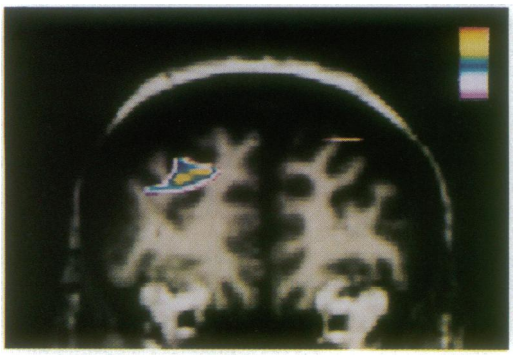

FIG. 4. Subject APE, second test session. Mean *t*-test image for Location task superimposed upon anatomical image.

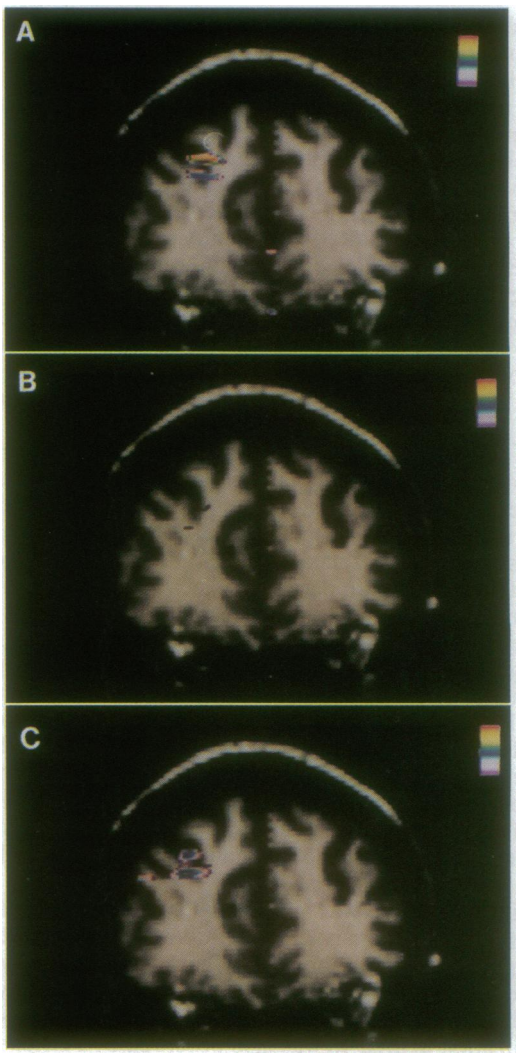

FIG. 5. (*A*) Grand mean *t*-test image for Location task across the five subjects restudied in the second test session showing activation in the right middle frontal region. These group data have been superimposed on a single subject's anatomical T_1-weighted image. (*B*) Corresponding grand mean *t*-test image for Color task across subjects showing minimal activation in the right middle frontal region. (*C*) Dot task grand mean *t*-test image showing coextensive activation to Location task *A*.

frontal gyrus was activated in the second session as in the first for Location. No consistent activation was seen in the cingulate region. Color showed only weak activation in a few voxels slightly ventral to the Location cluster. The activation for Dot (Fig. 5*C*) was overlapped with Location but had smaller magnitude. Again, Baseline yielded no activated clusters.

DISCUSSION

Performance of a spatial working memory task (i.e., the Location task) caused increased MR signal in the right middle frontal gyrus. This area, including Brodmann's area 46, has recently been remapped applying cytometric criteria and shown to be located on the middle frontal gyrus in the region activated in this study (P.G.R., unpublished work). This region was activated within 6–9 sec of task onset and declined slowly during the posttask interval. Some activation was also noted in the anterior cingulate and left middle frontal gyrus—areas interconnected with area 46 (21).

Potential sources of artifact from head movement, large blood vessels, and eye movements were investigated, and

runs contaminated by artifact were discarded. Cerebrospinal fluid suppression was used in the replication study to eliminate the bright cerebrospinal fluid signal outlining sulci that might result in edge artifacts with small movements. MR angiograms were acquired because it has been demonstrated that relatively large vessels on the brain surface can also give rise to functional effects. Within the resolution of the MR angiogram (1.5 mm^2), no vessels were apparent in the proximity of the observed ROIs. Proximity to the frontal eye fields (area 8) raised the concern that differential eye movements among the tasks could result in differential MR signal changes. A separate study was done with five subjects in which a blinded observer measured eye movements from an electrooculogram during three replications each of Location, Color, and Dot tasks. No significant differences were obtained in eye movements between tasks.

The activation observed for the Location task was greater across subjects than that obtained in the same regions in the two sensory-guided, target-detection tasks Color and Dot. Nevertheless, both caused significant activation, which in some subjects approached in magnitude that of the Location task. The Dot task, in particular, activated a region that, to the limits of our anatomical resolution, appeared to be coextensive with that for Location. This result is not surprising, given that sustained attention directed to peripheral spatial locations was also an essential component of the Dot task. Prefrontal neurons tuned to spatial stimuli are also recorded in and around area 46 (22). It is also possible that subjects were remembering the spatial locations of stimuli in the Color and Dot tasks despite instructions. The unblocked design may have encouraged this strategy. Additional studies are needed to separate the psychological factors contributing to the activation observed.

While activation was often bilateral (e.g., Fig. 2), the largest and most consistent activation occurred in the right hemisphere. We note, however, that inconsistent asymmetries in the signal strength of the shimmed images may have biased results in some subjects. Nevertheless, strong right lateralization in area 46 was also observed by Petrides *et al.* (8) in an experiment that required pointing to designs arranged in spatial locations. This asymmetry presumably reflects the right hemisphere's role in processing nonverbal, spatial material. The activation that we observed in midline areas (cingulate and superior frontal gyri) was also observed by Petrides *et al.* (8).

Our results differ from the PET study of Jonides *et al.* (11), who did not observe area 46 activation in a spatial working memory task but rather found inferior frontal activation in area 47. Petersen *et al.* (23) using PET, and McCarthy *et al.* (12) using fMRI, have shown activation of area 47 in word generation tasks. We did not observe activation of area 47, although the inferior aspects of our shimmed echo-planar images were affected by field inhomogeneities. We also did not observe consistent activation of area 9 as did Petrides *et al.* (8, 9), at least at the level of prefrontal cortex containing area 46.

There are limitations to the present study. While the single slice chosen for study allowed examination of areas 9, 46, 23, and often 47, it did not permit a detailed description of the anatomical extent of activation and did not include more posterior frontal (area 44) (10) and parietal (area 40) regions (10, 11), which have been reported to be activated in prior PET studies. Nevertheless, our results are consistent with prior PET studies (8, 9) and with a large corpus of human and monkey research (2, 3) in indicating the special role of mid-dorsolateral prefrontal cortex and area 46 in working memory tasks. We note that in a preliminary report (20), fMRI activation has also been observed in this region during performance of a *non*spatial working memory task. Whether these different tasks activate different regions of mid-dorsolateral prefrontal cortex remains to be determined. The fMRI technique has demonstrated sensitivity to the cognitive challenges reflected in working memory performance and should be of value in further elucidating the functional network responsible for this basic psychological process.

We thank Dr. Anthony Adrignolo, Francis Favorini, and Marie Luby for assistance in data analysis. This work was supported by the Department of Veterans Affairs, National Institute of Mental Health Grants MH-05286 and MH-44866, and National Institutes of Health Grant DK-34576.

1. Baddeley, A. (1992) *Science* **255**, 556–559.
2. Goldman-Rakic, P. S. (1987) in *Handbook of Physiology: The Nervous System*, ed. Plum, F. (Am. Physiol. Soc., Bethesda, MD), Vol. 5, pp. 373–417.
3. Fuster, J. (1973) *J. Neurophysiol.* **36**, 61–78.
4. Funahashi, S., Bruce, C. J. & Goldman-Rakic, P. S. (1989) *J. Neurophysiol.* **61**, 1–19.
5. Wilson, F. A. W., O'Scalaidhe, S. P. & Goldman-Rakic, P. S. (1993) *Science* **260**, 1955–1958.
6. Cavada, C. & Goldman-Rakic, P. S. (1989) *J. Comp. Neurol.* **287**, 422–445.
7. Mountcastle, V. B., Motter, B. C., Steinmetz, M. A. & Duffy, C. J. (1984) in *Dynamic Aspects of Neurological Function*, eds. Edelman, G. M., Gall, W. E. & Cowan, W. M. (Wiley, New York), pp. 159–193.
8. Petrides, M., Alivisatos, B., Evans, A. C. & Meyer, E. (1993) *Proc. Natl. Acad. Sci. USA* **90**, 873–877.
9. Petrides, M., Alivisatos, B., Meyer, E. & Evans, A. C. (1993) *Proc. Natl. Acad. Sci. USA* **90**, 878–882.
10. Paulescu, E., Frith, C. D. & Frackowiak, R. S. J. (1993) *Nature (London)* **362**, 342–345.
11. Jonides, J., Smith, E. E., Koeppe, R. A., Awh, E., Minoshima, S. & Mintun, M. A. (1993) *Nature (London)* **363**, 623–625.
12. McCarthy, G., Blamire, A. M., Rothman, D. L., Gruetter, R. & Shulman, R. G. (1993) *Proc. Natl. Acad. Sci. USA* **90**, 4952–4956.
13. Ogawa, S., Tank, D. W., Menon, R., Ellermann, J. M., Kim, S., Merkle, H. & Ugurbil, K. (1992) *Proc. Natl. Acad. Sci. USA* **89**, 5951–5955.
14. McCarthy, G., Blamire, A. M., Nobre, A. C., Puce, A., Hyder, F., Bloch, G., Phelps, E., Rothman, D. L., Goldman-Rakic, P. & Shulman, R. G. (1993) *Soc. Neurosci. Abstr.* **19**, 790.
15. Blamire, A. M., McCarthy, G., Nobre, A. C., Puce, A., Hyder, F., Bloch, G., Phelps, E., Rothman, D. L., Goldman-Rakic, P. & Shulman, R. G. (1993) *Soc. Magn. Reson. Med. Abstr.* **12**, 1413.
16. Talairach, J. & Tournoux, P. (1988) *Co-Planar Stereotaxic Atlas of the Human Brain* (Georg Thieme, Stuttgart).
17. Gruetter, R. & Boesch, C. (1992) *J. Magn. Reson.* **96**, 323–334.
18. Mansfield, P. (1977) *J. Phys. C.* **10**, L55–L58.
19. Blamire, A. M., Ogawa, S., Ugurbil, K., Rothman, D., McCarthy, G., Ellermann, J. M., Hyder, F., Rattner, Z. & Shulman, R. G. (1992) *Proc. Natl. Acad. Sci. USA* **89**, 11069–11073.
20. Cohen, J. D., Forman, S. D., Casey, B. J. & Noll, D. C. (1993) *Soc. Magn. Reson. Med. Abstr.* **12**, 1405.
21. Bates, J. F. & Goldman-Rakic, P. S. (1993) *J. Comp. Neurol.* **335**, 1–18.
22. Funahashi, S., Bruce, C. J. & Goldman-Rakic, P. S. (1993) *Biomed. Res.* **14**, 85–88.
23. Petersen, S. E., Fox, P. T., Posner, M. I., Mintun, M. & Raichle, M. E. (1988) *Nature (London)* **331**, 585–589.